

Article

Preparation and Electrical Properties of Insulation Paper Composed of SiO₂ Hollow Spheres

Ruijin Liao¹, Fuzhou Zhang^{1,*}, Yuan Yuan¹, Lijun Yang¹, Tuan Liu¹ and Chao Tang²

¹ State Key Laboratory of Power Transmission Equipment & System Security and New Technology, Chongqing University, Chongqing 400044, China; E-Mails: rjliao@cqu.edu.cn (R.L); yuany@cqu.edu.cn (Y.Y.); yljcqu@cqu.edu.cn (L.Y.); ltlyl100@126.com (T.L)

² College of Engineering and Technology, Southwest University, Chongqing 400700, China; E-Mail: tangchao_1981@163.com

* Author to whom correspondence should be addressed; E-Mail: zfzcqu@cqu.edu.cn; Tel.: +86-23-65106880; Fax: +86-23-65102442.

Received: 17 February 2012; in revised form: 2 July 2012 / Accepted: 16 July 2012 /

Published: 9 August 2012

Abstract: SiO₂ hollow spheres and low relative permittivity insulation paper handsheets composed of these SiO₂ hollow spheres with different weight percentages were successfully prepared. Low-content SiO₂ hollow spheres were uniformly dispersed in the insulation paper handsheets. The relative permittivity of the immersed oil Kraft-SiO₂ hollow sphere handsheets (K-SiO₂) initially decreased and then increased with increased amount of SiO₂ hollow spheres. K-5% SiO₂ possessed the lowest relative permittivity of approximately 1.68 at 50 Hz. The breakdown voltage of the paper-oil-paper composite insulation system increased from 26.4 kV to 30.5 kV with decreased relative permittivity of the paper from 2.55 to 1.68. The relationship between the relative permittivity and electric field strength of typical samples were also calculated.

Keywords: SiO₂ hollow spheres; relative permittivity; electrical properties; breakdown voltage

1. Introduction

Kraft, a form of cellulose insulation, is widely used in oil-filled transformer equipment [1–5]. Kraft is the preferred insulation for all oil-filled transformers because of its low cost and reasonably good performance. The relative permittivity of immersed oil Kraft is about 4.4, or more than twice that of

oil (2.1). Thus, the oil gap shares a higher electric field strength [6]. The electric field strength of the oil gap becomes lower if the relative permittivity of Kraft is reduced. Uniform electric field distributions can be achieved in paper-oil-paper composite insulation systems. Therefore, the insulating distance in transformers can also be decreased. In the previous work of our group, low relative permittivity polyimide (PI)-SiO₂ films were successfully prepared using SiO₂ hollow spheres with different weight percentages [7,8]. The relative permittivity of the composites decreased from 2.3 (pure PI) to 1.8, and then increased to 2.7.

In the present work, Kraft-SiO₂ hollow sphere insulation paper handsheets (K-SiO₂) were obtained. The distribution of the SiO₂ hollow spheres in the handsheets were observed by scanning electron microscopy (SEM). The effect of the content of the SiO₂ hollow spheres on the relative permittivity of the oil-immersed handsheets was investigated by broadband dielectric spectroscopy. The electric field distribution of a double-layer dielectric was calculated. Breakdown tests of the paper-oil-paper composite insulation system with different relative permittivity papers were also performed.

2. Preparation of SiO₂ Hollow Spheres and Low Relative Permittivity Handsheets

The SiO₂ hollow sphere powder was prepared by the method of Chen [2,7,9]. The powder was calcined at 500 °C for 6 h before use to remove any remaining polystyrene. The SiO₂ hollow spheres could be clearly observed. They were regular spheres about 500 nm in diameter (Figure 1a). The hollow structure of the spheres was confirmed by the breakage.

The SiO₂ hollow spheres were dissolved in deionized water (1:100 wt %) and the slurry was homogenized by vigorous agitation with a magnetic stir bar for 10 min. SiO₂ hollow spheres with different weight percentages were added to Kraft pulps. The mixtures were stirred for 3 min at 3000 r/min in a fiber disintegrating device, and were used to prepare the handsheets. Each wet handsheet was pressed at 15 MPa for 5 min at 80 °C, and dried at 105 °C for 7 min under a vacuum. Handsheets with a target basis weight of 120 g/m² were produced. SiO₂ hollow spheres with a low content were uniformly dispersed as almost individual particles in the matrix (Figure 1b). The SiO₂ hollow spheres locally aggregated with increased concentration (Figure 1c).

Figure 1. Scanning electron microscopy (SEM) images of (a) SiO₂ hollow spheres; (b) K-3% SiO₂, and (c) K-7% SiO₂.

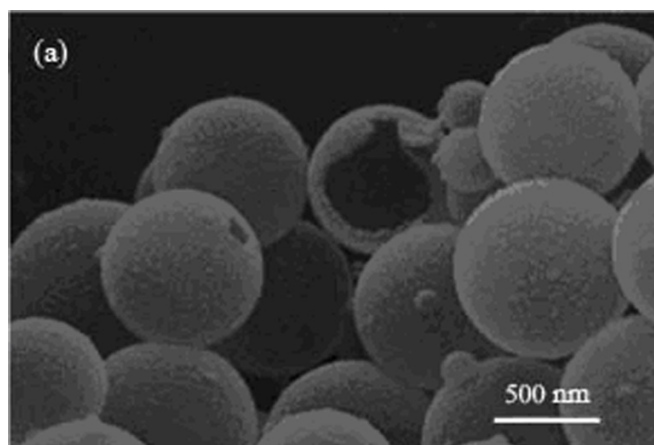
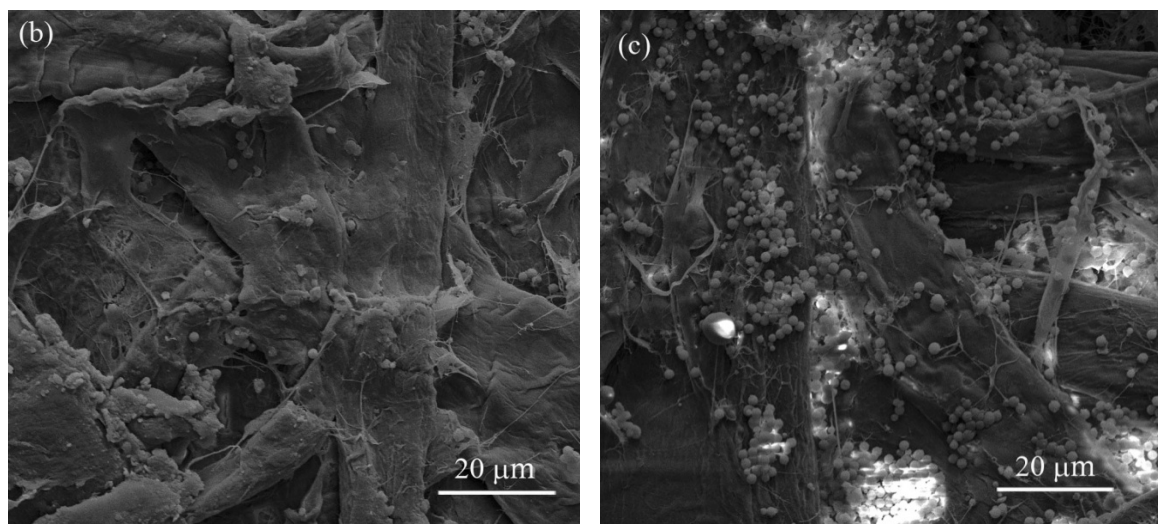


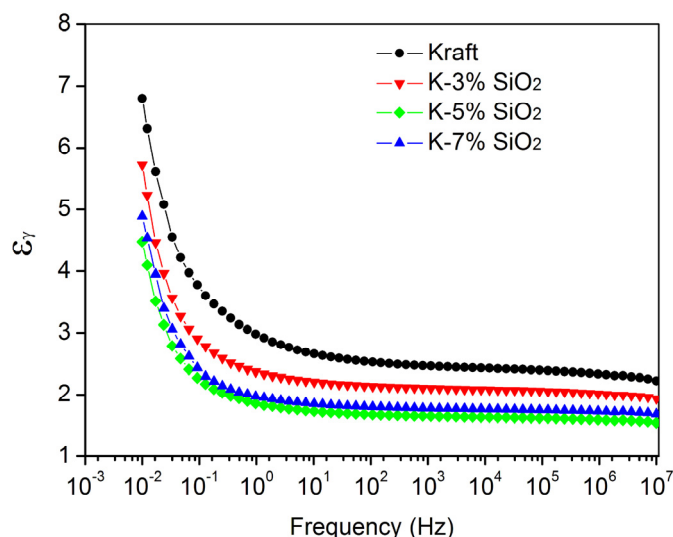
Figure 1. Cont.



The contents of SiO₂ hollow spheres in the handsheets were 0%, 3%, 5%, and 7%, and they were thus designated as Kraft, K-3% SiO₂, K-5% SiO₂, and K-7% SiO₂, respectively.

The relative permittivities of Kraft (immersed oil) composed of SiO₂ hollow spheres were tested at different frequencies ranging from 10⁻² Hz to 10⁷ Hz at 25 °C (Figure 2). The variation trends of the four samples were similar. The changes in the relative permittivities were moderate from 1 Hz to 10⁷ Hz, and dramatic under 1 Hz.

Figure 2. Effect of SiO₂ hollow sphere content on the relative permittivity of insulation paper.



The relative permittivities of the K-SiO₂ (K-3% SiO₂, K-5% SiO₂, and K-7% SiO₂) composites were lower than that of Kraft under different frequencies. The relative permittivity of air is 1.0. Thus, air voids stored in SiO₂ hollow spheres are one cause of reduced relative permittivity [10]. The existence of SiO₂ hollow spheres improves the distance of fiber chains. The oil content of handsheets increases due to air voids in the composites [11]. Therefore, the relative permittivity decreases [12–16]. Noticeably, the relative permittivity (at 50 Hz) of the composites decreased from 2.55 (Kraft) to 1.68

(K-5% SiO₂), and then increased to 1.95 (K-7% SiO₂). K-5% SiO₂ exhibited the lowest relative permittivity. A low content of SiO₂ hollow spheres (<5%) improved the distance of fiber chains. Thus, the relative permittivity decreased. A higher content of SiO₂ hollow spheres (7%) could fill the air voids in the composites; consequently, the air voids became smaller and the relative permittivity increased. The order of permittivity was Kraft > K-3% SiO₂ > K-7% SiO₂ > K-5% SiO₂.

The tensile strength of the handsheets was reduced with the addition of SiO₂ hollow spheres. The main reason was the existence of a weak interface between the fiber and SiO₂ hollow spheres. The tensile strengths of Kraft, K-3% SiO₂, K-5% SiO₂ and K-7% SiO₂ were 9.09 kN/m, 8.97 kN/m, 8.89 kN/m and 8.53 kN/m respectively. The tensile strength didn't show a sharp decline with K-SiO₂.

3. Double-Layer Dielectric Theory

The electric field strength of a double-layer dielectric is inversely proportional with the relative permittivity under an alternating current (AC) voltage. The electric field formula in a double-layer dielectric can be defined as:

$$E_1 = \frac{\varepsilon_2 U}{\varepsilon_1 d_2 + \varepsilon_2 d_1} \quad (1)$$

$$E_2 = \frac{\varepsilon_1 U}{\varepsilon_1 d_2 + \varepsilon_2 d_1} \quad (2)$$

where E_1 and E_2 are the electric fields of medias 1 and 2, respectively; U is the total electrical voltage; ε_1 and ε_2 are the relative permittivities of medias 1 and 2, respectively; and d_1 and d_2 are the thicknesses of medias 1 and 2, respectively.

Evidently, Equations (1) and (2) above are only suitable for two media. In the current experiment, although the paper-oil-paper composite insulation systems had three layers of media, these media were only of two kinds. Thus, the electric field strengths could be calculated using Equations (1) and (2). The thickness of the oil gap was designated as d_o (2, 3, and 4 mm). The relative permittivity of oil is 2.2; hence, the thickness of the paper was assumed to be 0.15 mm. The AC supply voltage was fixed at 100 kV.

The effect of the relative permittivity of the insulation paper on the electric field strength of the oil gap is shown in Figure 3. The variation trends in the different kinds of oil gaps were similar. The electric field strength of the oil gap decreased with decreased relative permittivity of the paper. However, under small thicknesses of the oil gap, the electric field strength of the oil gap significantly changed with the relative permittivity of the paper. When the relative permittivity of the paper decreased from 4 to 1 and the thicknesses of the oil gap d_o were 4, 3, and 2 mm, the electric field strength of the oil gap decreased by 10.6%, 13.6%, and 18.5%, respectively.

The effect of the relative permittivity of the insulation paper on its electric field strength is shown in Figure 4. The variation trends in the different kinds of oil gaps were also similar. The electric field strength of the insulation paper decreased with increased relative permittivity of the paper. However, under large thicknesses of the oil gap, the electric field strength of the insulation paper significantly changed with its relative permittivity. The distribution trend was opposite with that in Figure 3. When the relative permittivity of the paper decreased from 4 to 1 and the thicknesses of the oil gap d_o were

4, 3, and 2 mm, the electric field strength of the insulation paper increased by 257.6%, 245.4%, and 225.6%, respectively.

Figure 3. Effect of the relative permittivity of the insulation paper on the electric field strength (E_1) of the oil gap under three kinds of oil gap thicknesses.

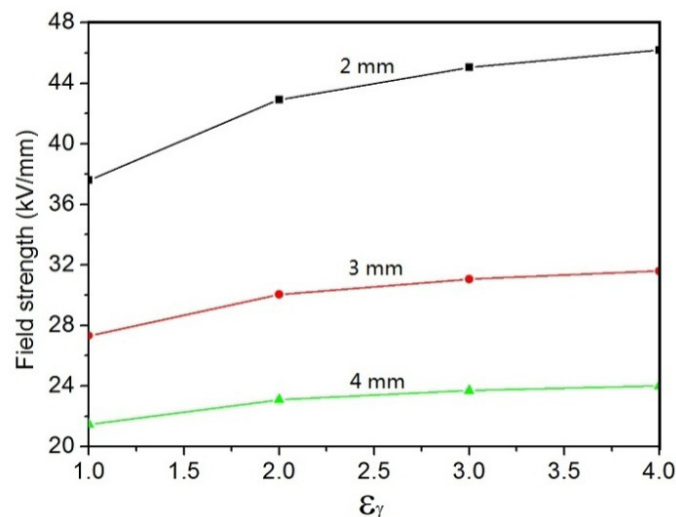
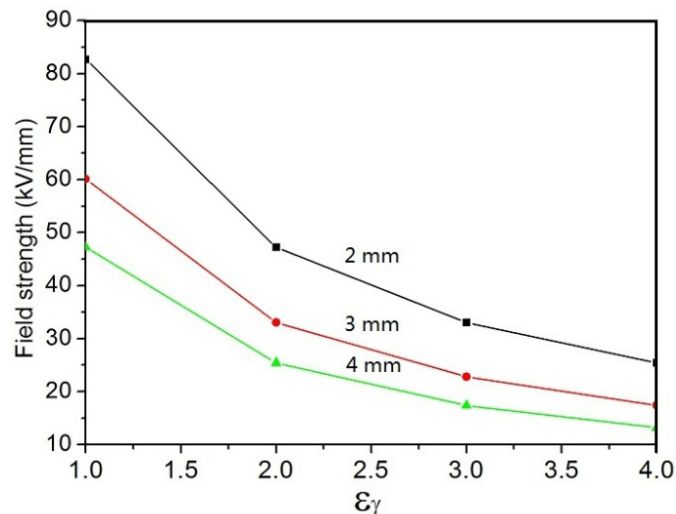


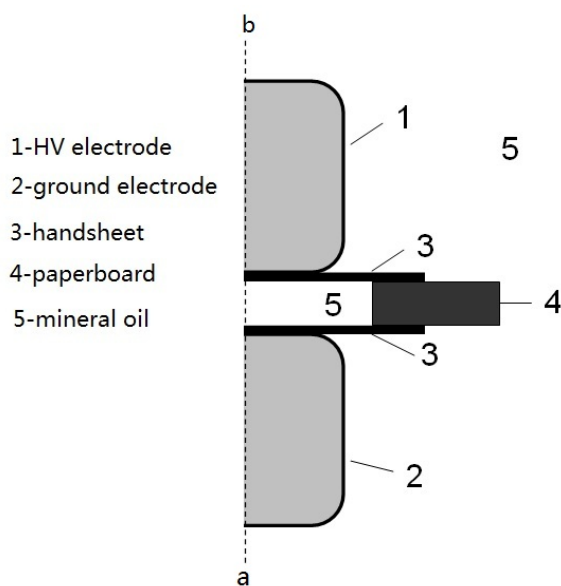
Figure 4. Effect of the relative permittivity of the insulation paper on its electric field strength (E_2) under three kinds of oil gap thicknesses.



4. Breakdown Experiment of a Paper-Oil-Paper Composite Insulation System

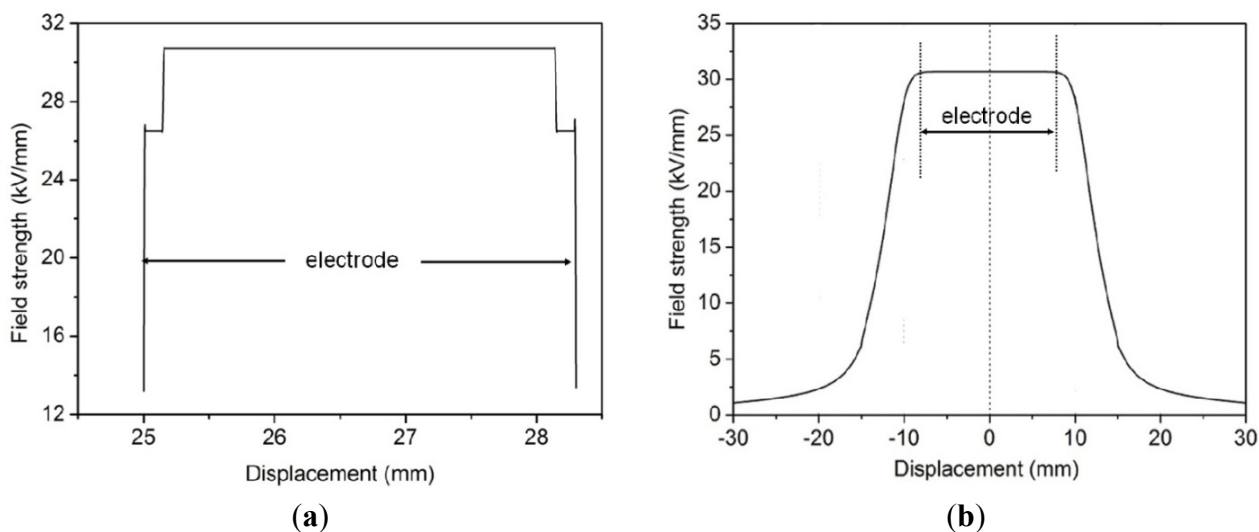
A uniformly distributed electric field between two test electrodes was proven by simulation analysis. Figure 5 depicts the computational domain for the dielectric test electrode. Line ab is the symmetry axis of electrode. The developed model was built under two-dimensional axial symmetry configurations and implemented using a COMSOL Multiphysics® package based on the finite element method. A sinusoidal voltage of 50 Hz with a peak value of 100 kV, was applied to the dielectric test setup.

Figure 5. Computational domain.



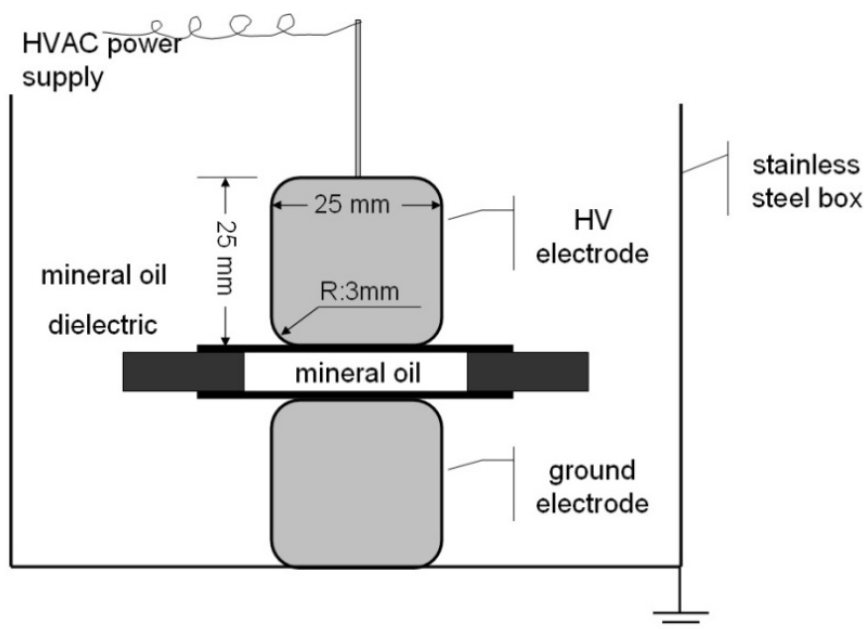
The electric field distribution between the two test electrodes is shown in Figure 6. The two test electrodes (Figure 5) had a range of 25 mm to 28.3 mm (Figure 6a) and -9.5 mm to 9.5 mm (Figure 6b). The electric field of paper or oil was uniform along the direction of line ab between the two test electrodes (Figure 6a). The curve (Figure 6b) shows the electric field distribution of oil along the vertical direction of line ab. The electric field distribution of paper along the vertical direction of line ab was in accordance with that in Figure 6b. Thus, the electric field of paper or oil was also uniform in the vertical direction of line ab between the two test electrodes. Therefore, the electric field distribution between the two test electrodes was uniform.

Figure 6. Electric field distribution: (a) line ab is the x-axis, and the bottom center of the ground electrode is the origin; (b) the vertical direction of line ab is the x-axis, and the center of the oil gap is the origin.



The diagram of the electrodes for measuring the breakdown voltage of the handsheets is shown in Figure 7. The diameter and height of the high-voltage (HV) and ground electrodes were both 25 mm. A copper bar was used to connect the HV electrode with the HV AC current power. In this test, mineral oil was used for the dielectric in the stainless steel box.

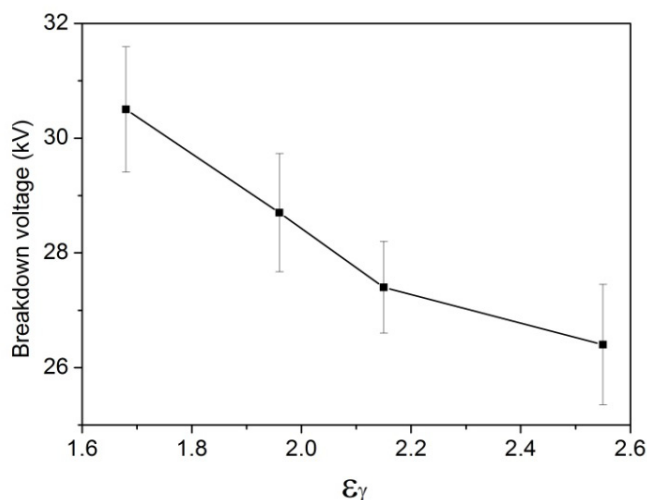
Figure 7. Diagram of electrodes.



The focus of the experiment was the effect of the relative permittivity on the breakdown voltage of the composite insulation system. Therefore, the thickness of the oil gap was only 3 mm. The oil gap was formed in the 3 cm-diameter hole of the 3 mm-thick paperboard. The external diameter of the paperboard was 6 cm. The thickness of the four kinds of experimental handsheet papers (Kraft, K-3% SiO₂, K-5% SiO₂, and K-7% SiO₂) were 0.15 mm in this experiment. Their relative permittivities at 50 Hz were 2.55, 2.15, 1.68, and 1.96, respectively. The handsheet papers were cut into 4 cm-diameter circles. All samples were put into the vacuum chamber and were dried at 90 °C for 48 h, and then the mineral oil at 40 °C was infused into the glass bottles in the vacuum chamber to immerse samples for 24 h. The moisture content of oil impregnated paper was 0.4% through such processing.

The effect of the relative permittivity of the handsheet on the breakdown voltage of the composite insulation system is shown in Figure 8. The breakdown voltage of the paper-oil-paper composite insulation system increased from 26.4 kV to 30.5 kV with decreased relative permittivity of the paper from 2.55 to 1.68.

Figure 8. Effect of the handsheet relative permittivity on the breakdown voltage of the composite insulation system.



5. Conclusions

SiO₂ hollow spheres and K-SiO₂ insulation paper handsheets composed of these SiO₂ hollow spheres with different weight percentages were synthesized. SiO₂ hollow spheres with a low content were uniformly dispersed. However, the SiO₂ hollow spheres locally aggregated with increased concentration. The relative permittivities of the immersed oil K-SiO₂ handsheets initially decreased and then increased with increased SiO₂ hollow sphere content. K-5% SiO₂ had the lowest relative permittivity. In the paper-oil-paper composite insulation system, the electric field strength of the oil gap decreased with decreased relative permittivity of the paper. However, the electric field strength of the insulation paper decreased with increased relative permittivity. Simulation analysis indicated that the electric field distribution between the two test electrodes was uniform. The breakdown voltage of the paper-oil-paper composite insulation system increased with decreased relative permittivity of the paper. The breakdown voltage of the composite insulation system increased from 26.4 kV to 30.5 kV when the relative permittivity of the paper decreased from 2.55 to 1.68. The experimental results were also consistent with the theoretically calculated data.

Acknowledgments

The authors acknowledge the Funds for Innovative Research Groups (51021005), China and the National Natural Science Foundation (50807054), China and Natural Science Foundation of Chongqing (2011M500132), China and Project the Fundamental Research Funds for the Central Universities (CDJZR12110018), China and the National Natural Science Foundation (Project for Young Scientists Fund, Grant No. 51107103), China.

References

1. Prevost, T.A.; Oommen, T.V. Cellulose insulation in oil-filled power transformers: Part I—History and development. *IEEE Electr. Insul. Mag.* **2006**, *22*, 28–35.

2. Deng, Z.W.; Chen, M.; Zhou, S.X.; You, B.; Wu, L.M. A novel method for the fabrication of monodisperse hollow silica spheres. *Langmuir* **2006**, *22*, 6403–6407.
3. Emsley, A.M.; Xiao, X.; Heywood, R.J.; Ali, M. Degradation of cellulosic insulation in power transformers. Part 2: Formation of furan products in insulating oil. *IEE Proc. Sci. Meas. Technol.* **2000**, *147*, 110–114.
4. Lundgaard, L.E.; Hansen, W. Aging of oil-impregnated paper in power transformers. *IEEE Trans. Power Deliv.* **2004**, *19*, 230–239.
5. Oommen, T.V.; Prevost, T.A. Cellulose insulation in oil-filled power transformers: Part II—Maintaining insulation integrity and life. *IEEE Electr. Insul. Mag.* **2006**, *22*, 5–14.
6. Kamata, Y.; Ohe, E.; Endoh, K.; Furukawa, S.; Tsukioka, H.; Maejima, M.; Fujita, H.; Nozaki, M.; Ishizuka, F.; Hyohdoh, K. Development of low-permittivity pressboard and its evaluation for insulation of oil-immersed EHV power transformers. *IEEE Trans. Electr. Insul.* **1991**, *26*, 819–825.
7. Yuan, Y.; Wang, Y.; Xie, B. Preparation and properties of polyimide/SiO₂ hollow spheres composite films with good dielectric property and amazing XRD spectra. *Optoelectron. Mater.* **2010**, *663*, 584–587.
8. Yuan, Y.; Lin, B.P.; Sun, Y.M. Novel low-dielectric-constant copolyimide thin films composed with SiO₂ hollow spheres. *J. Appl. Polym. Sci.* **2011**, *120*, 1133–1137.
9. Chen, M.; Wu, L.M.; Zhou, S.; You, B. A method for the fabrication of monodisperse hollow silica spheres. *Adv. Mater.* **2006**, *18*, 801–805.
10. Vo, H.T.; Shi, F.G. Towards model-based engineering of optoelectronic packaging materials: Dielectric constant modeling. *Microelectr. J.* **2002**, *33*, 409–415.
11. Wahab, M.A.; Kim, I.; Ha, C.-S. Microstructure and properties of polyimide/poly(vinylsilsesquioxane) hybrid composite films. *Polymer* **2003**, *44*, 4705–4713.
12. Kim, Y.B.; Yoon, K.-S. A physical method of fabricating hollow polymer spheres directly from oil/water emulsions of solutions of polymers. *Macromol. Rapid Commun.* **2004**, *25*, 1643–1649.
13. Lin, J.J.; Wang, X.D. Preparation, microstructure, and properties of novel low-kappa brominated epoxy/mesoporous silica composites. *Eur. Polym. J.* **2008**, *44*, 1414–1427.
14. Chung, C.L.; Hsiao, S.H. Novel organosoluble fluorinated polyimides derived from 1,6-bis(4-amino-2-trifluoromethylphenoxy) naphthalene and aromatic dianhydrides. *Polymer* **2008**, *49*, 2476–2485.
15. Lee, Y.-J.; Huang, J.-M.; Kuo, S.-W.; Chang, F.-C. Low-dielectric, nanoporous polyimide films prepared from PEO-POSS nanoparticles. *Polymer* **2005**, *46*, 10056–10065.
16. Hsiao, S.H.; Yang, C.P.; Chung, C.L. Synthesis and characterization of novel fluorinated polyimides based on 2,7-bis(4-amino-2-trifluoromethylphenoxy) naphthalene. *J. Polym. Sci. Part A Polym. Chem.* **2003**, *41*, 2001–2018.